

DdCBE mediates efficient and inheritable modifications in mouse mitochondrial genome

Jiayin Guo,^{1,2,6} Xiaoxu Chen,^{1,6} Zhiwei Liu,^{3,6} Haifeng Sun,^{1,6} Yu Zhou,¹ Yichen Dai,¹ Yu'e Ma,³ Lei He,³ Xuezhen Qian,¹ Jianying Wang,¹ Jie Zhang,³ Yichen Zhu,³ Jun Zhang,¹ Bin Shen,^{1,2,4,5} and Fei Zhou³

¹State Key Laboratory of Reproductive Medicine, Nanjing Medical University, Nanjing 211166, China; ²Gusu School, Nanjing Medical University, Nanjing 211166, China; ³Cambridge-Suda Genomic Resource Center, Jiangsu Key Laboratory of Neuropsychiatric Diseases Research, Medical College of Soochow University, Suzhou 215123, China; ⁴Center for Global Health, School of Public Health, Nanjing Medical University, Nanjing 211166, China; ⁵Women's Hospital of Nanjing Medical University, Nanjing Maternity and Child Health Care Hospital, Nanjing Medical University, Nanjing 211166, China

Critical mutations of mitochondrial DNA (mtDNA) generally lead to maternally inheritable diseases that affect multiple organs and systems; however, it was difficult to alter mtDNA in mammalian cells to intervene in or cure mitochondrial disorders. Recently, the discovery of DddA-derived cytosine base editor (DdCBE) enabled the precise manipulation of mtDNA. To test its feasibility for *in vivo* use, we selected several sites in mouse mtDNA as DdCBE targets to resemble the human pathogenic mtDNA G-to-A mutations. The efficiency of DdCBE-mediated mtDNA editing was first screened in mouse Neuro-2A cells and DdCBE pairs with the best performance were chosen for *in vivo* targeting. Microinjection of the mRNAs of DdCBE halves in the mouse zygotes or 2-cell embryo successfully generated edited founder mice with a base conversion rate ranging from 2.48% to 28.51%. When backcrossed with wild-type male mice, female founders were able to transmit the mutations to their offspring with different mutation loads. Off-target analyses demonstrated a high fidelity for DdCBE-mediated base editing in mouse mtDNA both *in vitro* and *in vivo*. Our study demonstrated that the DdCBE is feasible for generation of mtDNA mutation models to facilitate disease study and for potential treatment of mitochondrial disorders.

INTRODUCTION

Mitochondria, double-membraned subcellular organelles, function primarily to support aerobic respiration and produce ATP by oxidative phosphorylation.¹ Besides, mitochondria also participate in other cellular activities,^{2–5} including the production of endogenous reactive oxygen species (ROS), control of cytosolic calcium concentration, and apoptotic cell death. Mitochondrial functions are under dual genetic control by both nuclear and mitochondrial genomes. Most of the proteins required for mitochondria biogenesis and function are encoded within the nucleus.⁶ An independent mitochondrial genome (mtDNA) that encodes 37 genes is also of great importance. The double-stranded and circular mtDNA is continuously turned over, independently of the nuclear genome.⁷

Since the first pathogenic mtDNA mutation was identified in 1988,^{8,9} over 250 mtDNA mutations (point mutation and rearrangement)

have been characterized and connected with human diseases.^{10–14} mtDNA mutations are usually maternally inherited and can lead to diverse consequences, ranging from being phenotypically silent to causing critical diseases that generally affect multiple organs and systems. As cells generally contain several hundreds or thousands of mtDNA copies, mtDNA mutations are mostly heteroplasmic with heterogeneous phenotypes and also variable onset ages.¹⁵

As one of the most important model organisms for understanding mitochondrial pathology, the first heteroplasmic mouse model was generated by cytoplasmic fusion of two strains.^{16,17} Thereafter, the “Mito-mice” model was created by introducing mutant mtDNA into the zygote to mimic human symptoms.^{18,19} Similarly, other mice models with heteroplasmic mtDNA point mutations were also generated.^{20,21} Other mitochondria-related disease mouse models were also developed by manipulating nuclear genes that regulate mtDNA maintenance and replication (reviewed in Vempati et al.²² and Tynnismaa and Suomalainen²³).

Development of various mouse models helps promote our understanding of the functional consequences of mtDNA mutations and the molecular mechanisms of mitochondrial diseases progression. However, no curative treatments are currently available. Continuous efforts are being made to develop therapeutic approaches to reduce the copy number of pathogenic mutant mtDNA. DNA nucleases, such as zinc-finger nucleases and transcription activator–like effector nucleases (TALENs), have been genetically engineered to target and degrade mutant mtDNA.^{24,25} The CRISPR-Cas (clustered regularly interspaced short palindromic repeats associated with a Cas

Received 10 July 2021; accepted 16 November 2021;
<https://doi.org/10.1016/j.omtn.2021.11.016>

⁶These authors contributed equally

Correspondence: Jun Zhang, 101 Longmian Avenue, Nanjing 211166, China.

E-mail: zhang_jun@njmu.edu.cn

Correspondence: Bin Shen, 101 Longmian Avenue, Nanjing 211166, China.

E-mail: binshen@njmu.edu.cn

Correspondence: Fei Zhou, 199 Ren-ai Road, Suzhou Industrial Park, Suzhou 215123, China.

E-mail: fzhou@suda.edu.cn



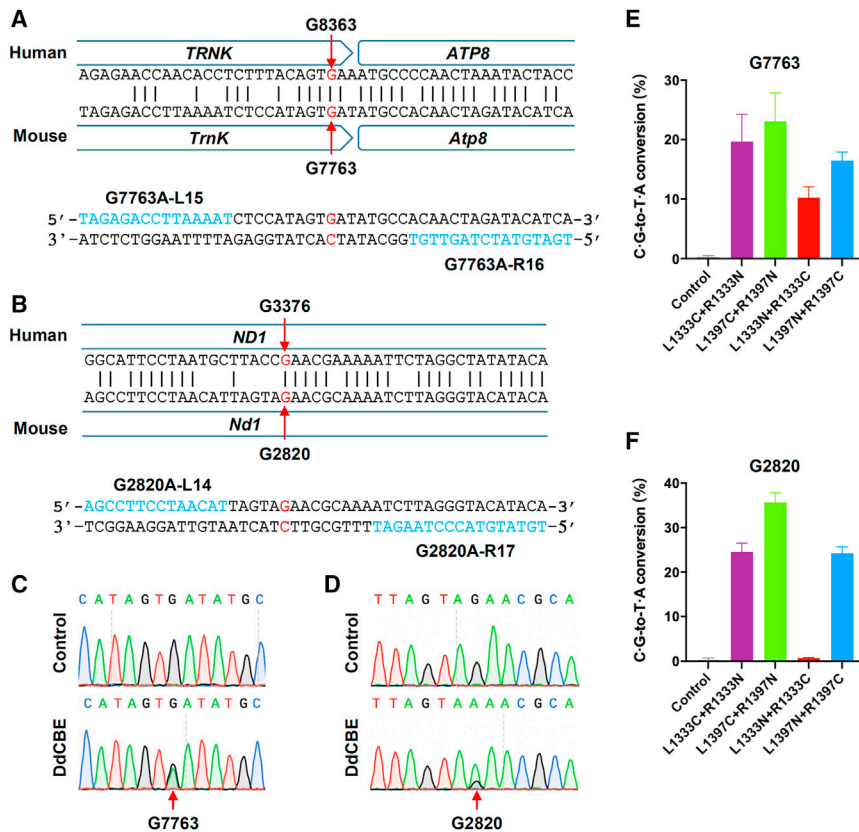


Figure 1. DdCBE-mediated m.G7763A and m.G2820A mutations in mouse N2A cells

(A and B) Sequence alignments indicate that mouse m.G7763 and m.G2820 are conserved with human m.G8363 and m.G3376, respectively. TALE targeting sequences are labeled in blue and the editing sites in red. (C–F) DdCBE-mediated editing efficiencies at m.G7763 (C and E) and m.G2820 (D and F) in mouse N2A cells. (C and D) Representative Sanger sequencing chromatograms of edited sites. (E and F) Deep sequencing analyses of editing efficiencies of different combinations of DdCBE pairs. Values and error bars reflect mean \pm SEM of $n = 3$ independent biological replicates.

units of NADH dehydrogenase and are essential for the electron transport chain. Human m.G8363A (mouse m.G7763A) and m.G8340A (mouse m.G7741A) are tRNA mutations that affect the mitochondrially encoded tRNA lysine (Table S1). These sites are confirmed pathogenic mtDNA mutations (Cfm status in MITOMAP) leading to multiple diseases including Leigh Disease, Leber Hereditary Optic Neuropathy (LHON), and myopathy in humans.¹⁰

First, mouse Neuro-2A (N2A) cells were used to test the efficiency of DdCBE-mediated mtDNA editing *in vitro*. DdCBEs were used to facilitate mouse m.G7763A and m.G2820A mutations

to resemble human m.G8363A and m.G3376A mutations, respectively (Figures 1A and 1B). DdCBE vectors were assembled by one-step Golden Gate assembly using an RVD library containing 192 vectors we developed before.²⁷ Transfection of DdCBE halves led to successful G-to-A conversion at both loci (Figures 1C and 1D). Deep sequencing data indicated that the combination of left-1397C with right-1397N achieved the highest editing efficiency for both m.G7763A (23.07% \pm 4.54%) and m.G2820A (35.63% \pm 2.18%) targeting (Figures 1E and 1F). Besides, mouse m.G12918A and m.G7741A mutations, resembling human m.G13513A and m.G8340A, were also tested, and similar results were obtained in N2A cells (Figures S1A–S1D). However, the left-1333C and right-1333N DdCBE pair seemed to be the optimal combination for both sites, as shown in the targeting efficiency by deep sequencing (Figures S1E and S1F). These results collectively demonstrate that DdCBE can facilitate efficient base editing at designated sites on the mtDNA of cultured mouse cells.

DdCBE-mediated mtDNA editing *in vivo*

The DdCBE pairs with the highest editing efficiency were then selected for *in vivo* targeting. DdCBE mRNAs were transcribed *in vitro*, purified, and injected into the mouse embryos. DdCBE mRNA concentrations at 25 ng/ μ L were initially injected at the one-cell stage for m.G7763A editing but no edited pups were obtained (Table 1). Higher concentrations of DdCBE mRNAs (100, 150, or

endonuclease) system and its derivative, Base Editor, are theoretically more powerful to correct the mutated point mutations but the requirement of guide RNAs prevents their use in mtDNA editing. Recently, the discovery of the toxin domain (DddA_{tox}, 1264–1427 amino acids) of a bacterial toxin deaminase (DddA), which catalyzes the deamination of cytidines within double-stranded DNA, provided a novel solution. DdCBE can facilitate precise and CRISPR-free manipulation of mtDNA²⁶; however, its delivery and editing efficiency need further verification *in vivo*.

In this study, we successfully generated mice with mutant mtDNA by microinjection of DdCBE pairs' mRNA, and proved that the mutations can be transmitted to the offspring maternally.

RESULTS

DdCBE-mediated mtDNA editing in mouse N2A cells

Mouse was used as the model to test the feasibility of using DdCBE to mimic human mtDNA pathogenic mutations. As categorized by the MITOMAP database, mtDNA disease mutations generally consist of two types: rRNA/tRNA mutations and Coding & Non-Coding/Control Region mutations. By comparing human and mouse mtDNA sequences, we selected four human mtDNA G-to-A mutations as our targeting candidates. Human m.G3376A (mouse m.G2820A) and m.G13513A (mouse m.G12918) mutations affect the coding region of *MT-ND1* and *MT-ND5* genes respectively. *MT-ND1* and *MT-ND5* encode sub-

Table 1. DdCBE injection summary

Site	Time of injection	Concentration of DdCBE mRNAs (ng/ μ L)	Number of transplanted embryos	Total pups (rate)	Live pups	Number of edited pups (rate)	Base conversion rate
m.G7763A	1-cell embryo	25	107	51 (0.48)	51	0 (0)	0
		100	50	14 (0.28)	14	5 (0.35)	2.48%–16.42%
		150	48	22 (0.46)	22	5 (0.23)	8.49%–15.38%
		200	141	33 (0.23)	32	13 (0.41)	5.76%–18.51%
	2-cell embryo	150	57	5 (0.09)	4	1 (0.25)	11.20%
		200	21	8 (0.38)	8	1 (0.125)	6.94%
m.G2820A	1-cell embryo	150	52	29 (0.56)	28	16 (0.57)	3.02%–14.33%
		200	25	13 (0.52)	12	3 (0.25)	6.51%–7.38%
	2-cell embryo	150	49	20 (0.51)	18	6 (0.33)	4.54%–23.50%
		200	26	8 (0.31)	8	2 (0.25)	25.36%–28.51%
m.G12918A	1-cell embryo	150	53	11 (0.21)	9	3 (0.33)	3.52%–19.09%
m.G7741A	1-cell embryo	150	45	13 (0.29)	13	6 (0.46)	3.09%–13.26%

200 ng/ μ L) were then injected at the one-cell or two-cell stage. As a result, 25 of 80 live pups for m.G7763A and 27 of 66 for m.G2820A were found successfully edited (Figures 2A and 2B; Table 1). The base conversion rate in edited pups ranged from 2.48% to 18.51% for m.G7763A and from 3.02% to 28.51% for m.G2820A (Figures 2C and 2D; Table 1). Successfully edited pups for m.G12918A (3/9) and m.G7741A (6/13) were also obtained with conversion rates ranging from 3.52% to 19.09% and from 3.09% to 13.26%, respectively (Figure S2; Table 1).

To further characterize the editing status in founder mice, we killed two female founders (G7763-F0-3# and 12#) at the 4-week stage and collected major tissues, as well as oocytes from the ovary. Deep sequencing results indicated that the G-to-A conversion rates were comparable throughout the mouse body (Figures 2E and S3). Interestingly, the mutation load in different oocytes was variable (Figure 2F), suggesting that higher mutation loads may be obtained in F1 offspring than that in founders. Together, these findings indicate that injection of DdCBE mRNAs in early embryos can achieve systemic mtDNA editing, including in the germ cells.

Germline transmission of DdCBE-mediated mtDNA mutation

To investigate whether the DdCBE-mediated mtDNA mutation is inheritable, we backcrossed female m.G7763A and m.G2820A founders with wild-type male mice and obtained F1 offspring. Either m.G7763A or m.G2820A mutations can be detected in corresponding F1 offspring (Figures 3A and 3B), demonstrating that DdCBE-mediated mtDNA mutations can be transmitted to the next generation.

Consistent with the results obtained in the oocytes of the edited female founder, deep sequencing results indicated that F1 offspring harbored different levels of mutation loads and some were even higher than the founder (Figures 3C and 3D). For example, the female founder 9# harboring 12.04% m.G7763A mutation generated

offspring with mutation loads ranging from 5.95% to 27.96% (Figure 3C; Table 2). The variation of the mutation loads in F1 offspring suggests that it is theoretically possible to obtain individuals with mutation loads high enough to display phenotypes in future generations. Indeed, by choosing to breed F1 offspring with relatively high mutation loads, we could obtain F2 offspring with mutation loads up to 50% (Figure S4).

DdCBE-mediated off-target editing in mtDNA

To assess the off-target activity of DdCBE in the mouse mitochondrial genome, we analyzed the deep sequencing data to find DdCBE-induced single-nucleotide variants (SNVs) around the on-target sites. In N2A cells, C•G-to-T•A conversion could be detected in the spacing region and nontarget sites (Figures S5A–S5D). In the spacing region, DdCBE pairs yielded bystander mutations with variable editing efficiency; for example, the m.G7763A DdCBE pair yielded 0.03% \pm 0.006% to 6.7% \pm 0.67% editing (Figure S5A), and the m.G7741A DdCBE pair yielded 0.02% \pm 0.006% to 25.38% \pm 3.10% editing (Figure S5D). Notably, C within 5'-aC and 5'-acC contexts could be converted to T, with efficiency up to 25.38% \pm 3.10% and 23.64% \pm 3.67%, respectively (Figures S5A–S5D), indicating DddA_{tox} also attacked these two motifs besides the 5'-tC motif in the spacing region. However, in nontarget sites, all off-target SNVs only occurred within the 5'-tC motif, suggesting that the off-target editing indeed arose from DddA_{tox}, which preferred the 5'-tC motif during transient reassembly at off-target sites, rather than the 5'-aC and 5'-acC motifs. At these sites, off-target editing rate was below 1% in most cases with exceptions where certain DdCBE combinations showed off-target rates higher than 3% at m.C12809 (Figure S5C).

To model the human pathogenic mtDNA mutations precisely, high-performance DdCBE pairs with lower off-target activity and less bystander mutation in the spacing region were selected to generate mice. Deep sequencing results of the F0 pups indicated that the

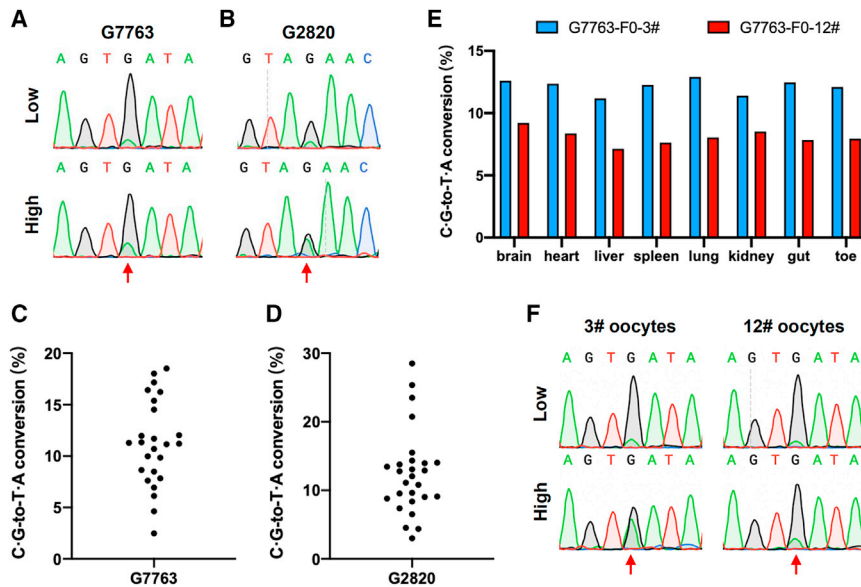


Figure 2. DdCBE-mediated m.G7763A and m.G2820A mutations *in vivo*

(A and B) Representative Sanger sequencing chromatograms of low (upper) and high (lower) base conversion rate in m.G7763A (A) and m.G2820A (B) founder mice. (C–D) Base conversion rate of edited mice obtained through microinjections of DdCBE targeting m.G7763 (C, $n = 25$) and m.G2820 (D, $n = 27$). (E) Deep sequencing analyses of the base conversion rates in different tissues of m.G7763A edited founder mice 3# (blue) and 12# (red). (F) Representative Sanger sequencing chromatograms of low (upper) and high (lower) mutation loads in oocytes of m.G7763A edited founder mice 3# (left) and 12# (right).

undesired editing in the spacing region was less than 0.5% in m.G7763A and m.G12918A founders (Figures 4A and 4C), while in the m.G2820A and m.G7741A founders, the undesired editing efficiency was up to 6.1% and 13.56%, respectively (Figures 4B and 4D). At off-target sites, the editing rates were mostly below 1% except at the m.C7854 site in a few of m.G7763A founders (Figure 4A). Deep sequencing analyses were also performed for potential off-target sites (OTs) in nuclear DNA where the sequences were completely identical to on-target mtDNA sites. As a result, no off-target edits were detected at these nuclear loci, indicating that DdCBE-mediated editing was mtDNA-specific (Figure S6). To further evaluate the off-target activity of DdCBE on the entire mitochondrial genome, we performed whole mtDNA sequencing in m.G7763A and m.G2820A founders. The results showed that only a few sites were detected with less than 2% of off-target editing, and almost all of these OTs were concentrated near the target sites, indicating that these off-target editings may be induced by the unstable binding of the DdCBE pair (Figure 5). In addition, the sparse off-target events could also be detected along the whole mtDNA, which may be caused by sequence-independent activity of DdCBE.

In summary, except for the bystander mutations in spacing regions, DdCBE overall exhibits a high targeting fidelity and can mediate precise base editing in mouse mtDNA with limited off-target editing.

DISCUSSION

We have demonstrated in this study that DdCBE-mediated mtDNA editing is feasible for generating inheritable mtDNA mutations. As the overall targeted base conversion rates in F0 founder mice were limited, we speculated that this was mainly affected by the suspension of mtDNA replication in the early embryonic stage. In humans, mtDNA replication is critically downregulated from the fertilized oocyte through the pre-implantation embryo.²⁸ Similarly, the murine oocytes possess more than 100,000 mtDNA copies before fertilization

but this number does not increase until post-implantation.^{29,30} Because DdCBE-mediated base substitution relies on the repairing process after deamination, suspended mtDNA replication in early embryonic stages will theoretically impair the editing outcome. Meanwhile, the number of mtDNA copies and the half-life of injected mRNAs may also impact the editing results. We tried to inject different concentrations of DdCBE mRNAs but no concentration-dependent improvement of editing efficiency was observed. However, obvious toxicity of DdCBE mRNAs was noticed when high injection concentrations (200 ng/ μ L) were used (Table S2), which can be concluded from the decreased birth rate in this study and also a recent report in which a total concentration of 600 ng/ μ L mRNAs were injected.³¹ Moreover, we also performed microinjection at the two-cell stage in order to sustain DdCBE mRNA to later stage but the results in different tests were not consistent. Different experimental conditions need to be further tested in the future to determine whether there is an efficiency plateau for DdCBE-mediated mtDNA editing in mouse embryos. Overall, the base conversion rate in the F0 founders and mutation load in F1 offspring were probably not enough to cause disease phenotypes due to the “threshold effect.” However, heteroplasmic mtDNA generally resulted in offspring with distinct mutation loads due to mitochondrial genetic bottleneck.³² The observation of variable mutation loads in F1 and F2 offspring indicated the possibility if getting progeny with mutation loads high enough to exhibit clinically relevant disorders. In that case, these mutant mice could be used as disease models for pathogenesis studies and therapeutic development.

Unlike the previous report,³¹ comprehensive off-target analyses were performed in this study. During off-target analyses, we noticed that C·G-to-T·A conversion can also be detected at quite high frequencies in spacing regions with certain DdCBE pairs. Further characterization discovered two novel motifs for DddA_{tox} recognition: 5'-aC and 5'-acC. Although these motifs seemed to be functional only in spacing regions, they could be used in certain scenario to expand the targeting availability for DdCBE. On the contrary, undesired editing at these motifs can also be largely avoided by selecting appropriate DdCBE pairs. This finding somehow broadened

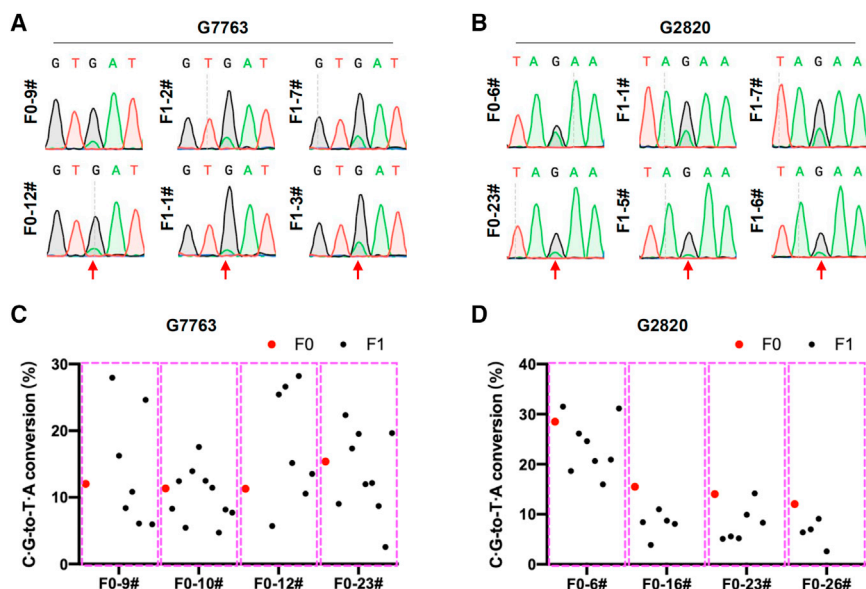


Figure 3. Germline transmission of m.G7763A and m.G2820A mutations

(A and B) Representative Sanger sequencing chromatograms of m.G7763A (A) and m.G2820A (B) founder mice and their offspring. (C and D) Deep sequencing analyses of the base conversion rate and mutation loads in m.G7763A (C) and m.G2820A (D) founder mice and their offspring. Results of the founder and its F1 offspring are shown in the same box. Red dots: founder; black dots: F1 offspring.

our knowledge of DddA_{tox} and could guide us to use DdCBE for mtDNA editing in a more accurate way. Based on its targeting capability and specificity, DdCBE also could be used for potential clinical treatment of mitochondrial disorder caused by A•T-to-G•C mutation (e.g., human m.A3260G, m.A4300G, m.T7510C, m.T7511C, m.T8356C, m.A14495G, etc.). By targeted base editing, the disease-causing mutation load theoretically can be reduced to below the "threshold" to achieve a therapeutic result. To validate its potential for gene therapy, we designed DdCBE pairs targeting a pathogenic mutation A4300G, which is associated with human hypertrophic cardiomyopathy.³³ As a result, G-to-A conversion could be achieved efficiently in cells (Figure S7). A series of validation studies focusing on the therapeutic application of DdCBE are expected to emerge in the future.

Regardless of its efficiency and precision, the application of DdCBE to generate mtDNA mutation is still limited up to now. More extensive mtDNA editing requires the development of other versions of editors

Table 2. Germline transmission of mtDNA mutations

Mutation	Founder mouse	F0 base conversion rate (%)	Number of F1 offspring	Number of mutant F1	Mutation load of mutant F1 (%)
m.G7763A	9#	12.04	7	7	5.95–27.96
	10#	11.34	10	10	4.7–17.56
	12#	11.29	7	7	5.71–28.20
	23#	15.38	9	9	2.55–22.34
m.G2820A	6#	28.51	9	9	15.97–31.53
	16#	15.51	5	5	3.87–11.00
	23#	14.04	6	6	5.09–14.16
	26#	12.05	4	4	2.58–9.09

that rely on the discovery of new DddA_{tox}-like toxins with different deaminase activity. Similar to the conventional base editor system, we believe that the mtDNA editing tool will also evolve rapidly and its application will be greatly expanded in the near future.

MATERIALS AND METHODS

Plasmid construction

DdCBE vectors were assembled using RVD libraries as before.²⁷ The complete set of plasmids for assembling DdCBE can be obtained from Addgene (pending). In brief, RVDs and backbone plasmids were digested with Bsa I and ligated with T4 DNA ligase in a single reaction using the following program: 37°C for 10 min; 10 cycles of 10 min at 37°C and 10 min at 16°C; 50°C for 5 min; 80°C for 5 min. The assembled plasmids were chemically transformed into *Escherichia coli* DH5 α (Transgene), and then confirmed by PCR and Sanger sequencing.

Cell culture and nucleofection

N2A cells (ATCC, CCL-131) were maintained in DMEM supplemented with 10% FBS (Gemini) at 37°C with 5% CO₂, and detected without mycoplasma contamination by PCR test; 400 ng of the DdCBE pair was nucleofected with 4D-Nucleofector (Lonza) according to the manufacturer's protocol using SF Cell Line 4D-Nucleofector X Kit. The nucleofected cells were seeded onto the 12-well plate and supplemented with 2 μ g/mL puromycin 24 h post nucleofection; 96 h later, cells were collected for DNA extraction.

In vitro transcription of DdCBE

DdCBE plasmids containing a T7 promoter were linearized with Pme I (New England Biolabs) and transcribed using mMESAGE mMACHINE T7 Ultra Kit (Life Technologies) according to the manufacturer's manual. Transcribed RNA was purified by RNA Clean & Concentrator-5 (Zymo Research) and stored at –80°C until use.

Mouse

For microinjection, C57BL/6N and ICR mice were used as embryo donors and foster strain, respectively. All mice were housed and bred in a specific pathogen-free barrier facility of Soochow University with normal diet and 12:12-h light/dark cycle. Related experiments were reviewed and approved by the Institutional Animal Care and

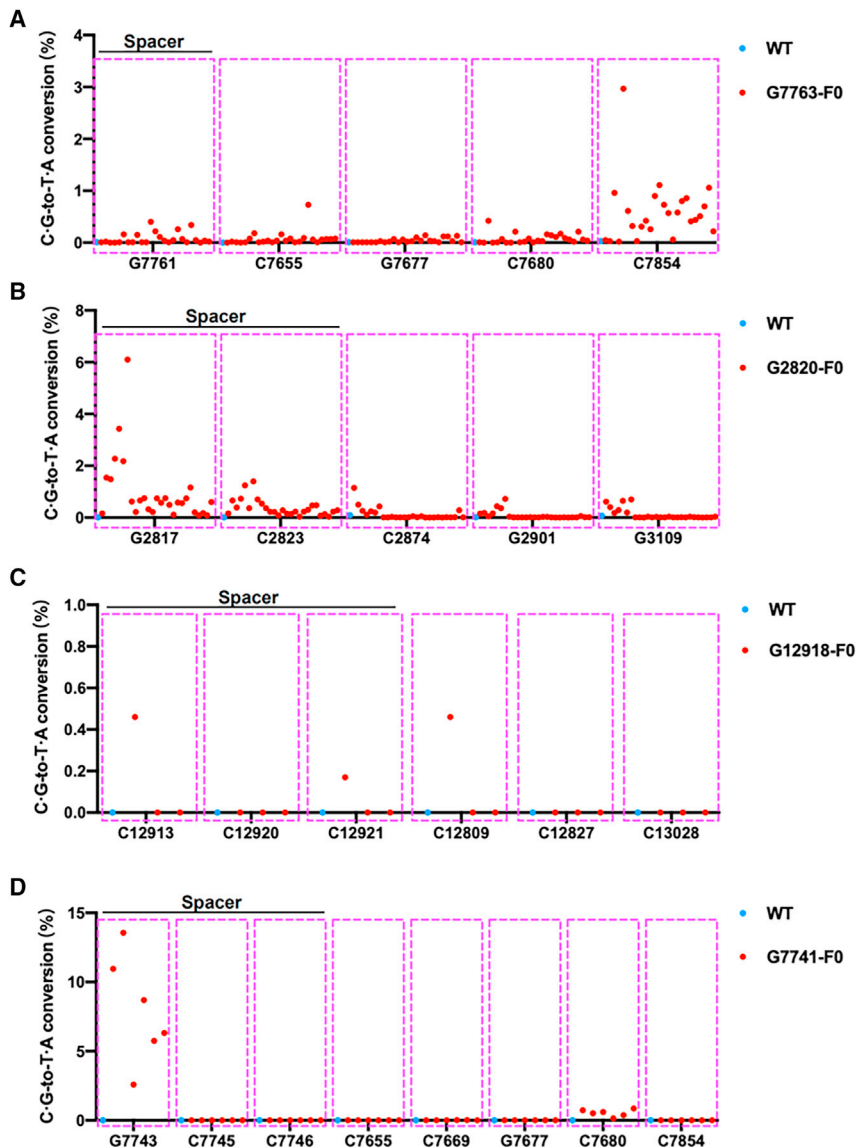


Figure 4. Off-target editing by DdCBE *in vivo*

(A–D) Deep sequencing analyses of off-target editing rates in m.G7763A (A), m.G2820A (B), m.G12918A (C), and m.G7741A (D) founder mice (red dots) with wild-type mice as control (blue dots). Each dotted box indicates a single off-target site.

mice. For *in vitro* analysis, injected embryos were culture in KSOM medium (Sigma) and the ratio of embryos developing to blastocyst (blastocyst efficiency) was used to evaluate the toxicity of injected DdCBE mRNA.

DNA extraction and genotyping

The genomic DNA of N2A cells and mouse tissues was extracted by QuickExtract DNA Extraction Solution (Lucigen). In detail, samples were incubated at 65°C for 45 to 60 min to release the DNA and further incubated at 98°C for 2 min. The lysate was used as a PCR template. Signal oocyte was directly used as PCR template without lysis. The targeted fragments spanning the editing sites were amplified for Sanger sequencing. Primers are listed in the Table S3.

Whole mtDNA sequencing

Whole mtDNA was captured by long-range PCR as previous reported.²⁶ Two overlapping mtDNA fragments around 8 kb each were purified by gel extraction and subjected to construct sequencing libraries using TruePrep DNA Library Prep Kit V2 for Illumina (Vazyme). The libraries were purified using DNA Clean beads by 0.5×/0.35× double-size selection. Libraries were pooled and sequenced by Illumina NovaSeq platform.

Deep sequencing

The first round PCR (PCR1) was conducted with barcoded primers to amplify the genomic region

of interest using Phanta Max Super-Fidelity DNA Polymerase (Vazyme). The products of PCR1 were pooled with equal moles and purified for the second round PCR (PCR2). The PCR2 products were amplified using index primers (Vazyme) and purified by gel extraction for sequencing using the Illumina NovaSeq platform. Barcoded primers used in PCR1 are listed in Table S3.

Deep sequencing data analysis

The mouse mitochondrial genome reference sequence (NC_005,089) was downloaded from the NCBI database. Bowtie2 was used to build the alignment index using default parameters. Paired end reads with overlap were merged into a single read using homemade scripts, and bowtie2 was used for alignment in single end mode. Otherwise, reads were mapped in paired end mode by using bowtie2 with default

Use Committee of Cambridge-Suda Genomic Resource Center, Soochow University.

Microinjection

Female C57BL/6N mice (about 4 weeks old) were superovulated by intraperitoneally injecting pregnant mare serum gonadotropin (PMSG) at Day –3 and chorionic gonadotropin (HCG) at Day –1. Immediately after HCG injection, female mice were mated with male C57BL/6N mice. Female mice were killed the next day and zygotes (E0.5) were collected from oviducts. Harvested zygotes were directly injected or cultured overnight *in vitro* to the two-cell stage for microinjection. DdCBE mRNA was injected into zygote cytoplasm or one blastomere of the two-cell embryo. Injected embryos were transferred into the oviduct of pseudopregnant ICR female

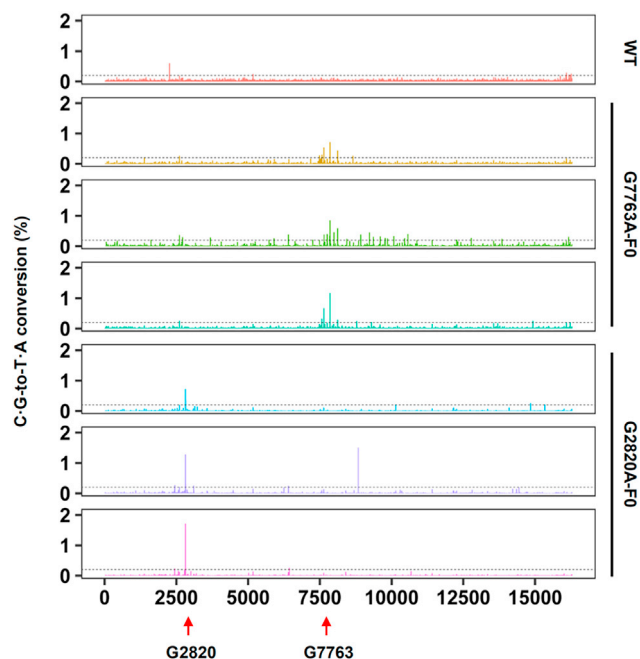


Figure 5. Off-target editing by DdCBE on entire mitochondrial genome. Whole mtDNA sequencing of m.G7763A and m.G2820A founder mice.

parameters. Alignment results were converted to bam format using samtools and visualized in Integrative Genomics Viewer. Bases with phred quality score greater than 30 ($Q > 30$) were kept for further analyses, and bases with depth over 2 million were truncated to 2 million. Only C-to-T or G-to-A conversion was calculated for DdCBE-mediated editing.

Whole mtDNA sequencing data analysis

Quality control was performed by using fastqc and trim_galore in the paired end mode. The Illumina adapter sequence or Ns in either side of the read was trimmed, and only reads with quality over 20 were kept for further analysis. QC-passed reads were mapped to NC_005089 using bowtie2 with default parameters. Editing events in the nontarget region were considered as putative off-targets.

Off-target analysis

SNP sites of mouse mtDNA were obtained from the Ensembl database, which includes 33 annotated C•G-to-T•A variations. For the off-target analysis on whole mtDNA, the following sites were excluded before analysis and visualization: (1) the above obtained SNP sites; (2) the evident SNP sites with C•G-to-T•A variation over 90% in any sample; (3) sites within the DdCBE spacing region. OTSs in the nuclear genome were first predicted by blasting mitochondrial on-target sequences against the nuclear genome. Nuclear loci completely homologous with targeted mitochondrial sequences were selected for deep sequencing. The putative OTSs were amplified and sequenced by the Hi-TOM platform.³⁴ Primers are listed in Table S3.

DATA AVAILABILITY

The high-throughput sequencing data have been deposited to the NCBI Sequence Read Archive database under the accession ID PRJNA716542 (SRA: PRJNA716542).

SUPPLEMENTAL INFORMATION

Supplemental information can be found online at <https://doi.org/10.1016/j.omtn.2021.11.016>.

ACKNOWLEDGMENTS

This work was supported by the National Key R&D Program of China (2018YFA0801100 and 2016YFC1000600), the National Natural Science Foundation of China (31970796, 31871445), the Science and Technology Project of Jiangsu Province (BZ2020067), and the Special Foundation of National Human Genetic Resource Sharing Service Platform (YCZYPT[2020]08). We thank the staffs of the animal facility for their support of the study.

AUTHOR CONTRIBUTIONS

B.S., F.Z., and J.Z. conceived the project and designed the experiments. J.G. and X.C. performed all sequencing work and cell work, and analyzed the data. Z.L. led the mouse production with the help of Y.M. and L.H. H.S. performed all computational analyses. Y.Z., Y.D., and J.W. generated the TALE library and constructed DdCBE vectors with the help of X.Q. J.Z. and Y.Z. performed the mouse sample collection. F.Z. and B.S. wrote the manuscript with inputs from all authors.

DECLARATION OF INTERESTS

The authors declare no competing interests.

REFERENCES

- Hatefi, Y. (1985). The mitochondrial electron transport and oxidative phosphorylation system. *Annu. Rev. Biochem.* 54, 1015–1069.
- Pozzan, T., Magalhaes, P., and Rizzuto, R. (2000). The comeback of mitochondria to calcium signalling. *Cell Calcium* 28, 279–283.
- Newmeyer, D.D., and Ferguson-Miller, S. (2003). Mitochondria: releasing power for life and unleashing the machineries of death. *Cell* 112, 481–490.
- Starkov, A.A. (2008). The role of mitochondria in reactive oxygen species metabolism and signaling. *Ann. N. Y. Acad. Sci.* 1147, 37–52.
- Scheffler, I.E. (2007). Metabolic pathways inside mitochondria. In *Mitochondria*, Second edition. John Wiley & Sons, pp. 298–344.
- Wallace, D.C. (2005). A mitochondrial paradigm of metabolic and degenerative diseases, aging, and cancer: a dawn for evolutionary medicine. *Annu. Rev. Genet.* 39, 359–407.
- Bogenhagen, D., and Clayton, D.A. (1977). Mouse L cell mitochondrial DNA molecules are selected randomly for replication throughout the cell cycle. *Cell* 11, 719–727.
- Holt, I.J., Harding, A.E., and Morgan-Hughes, J.A. (1988). Deletions of muscle mitochondrial DNA in patients with mitochondrial myopathies. *Nature* 331, 717–719.
- Wallace, D.C., Singh, G., Lott, M.T., Hodge, J.A., Schurr, T.G., Lezza, A.M., Elsas, L.J., and Nikoskelainen, E.K. (1988). Mitochondrial DNA mutation associated with Leber's hereditary optic neuropathy. *Science* 242, 1427–1430.
- (2019). MITOMAP: a human mitochondrial genome database. <http://www.mitomap.org>.
- Greaves, L.C., and Turnbull, D.M. (2009). Mitochondrial DNA mutations and ageing. *Biochim. Biophys. Acta* 1790, 1015–1020.

12. Park, C.B., and Larsson, N.G. (2011). Mitochondrial DNA mutations in disease and aging. *J. Cell Biol.* *193*, 809–818.
13. Reeve, A.K., Krishnan, K.J., and Turnbull, D. (2008). Mitochondrial DNA mutations in disease, aging, and neurodegeneration. *Ann. N. Y. Acad. Sci.* *1147*, 21–29.
14. Santos, C., Martinez, M., Lima, M., Hao, Y.J., Simoes, N., and Montiel, R. (2008). Mitochondrial DNA mutations in cancer: a review. *Curr. Top. Med. Chem.* *8*, 1351–1366.
15. McFarland, R., Taylor, R.W., and Turnbull, D.M. (2007). Mitochondrial disease—its impact, etiology, and pathology. *Curr. Top. Dev. Biol.* *77*, 113–155.
16. Jenuth, J.P., Peterson, A.C., Fu, K., and Shoubridge, E.A. (1996). Random genetic drift in the female germline explains the rapid segregation of mammalian mitochondrial DNA. *Nat. Genet.* *14*, 146–151.
17. Jenuth, J.P., Peterson, A.C., and Shoubridge, E.A. (1997). Tissue-specific selection for different mtDNA genotypes in heteroplasmic mice. *Nat. Genet.* *16*, 93–95.
18. Inoue, K., Nakada, K., Ogura, A., Isobe, K., Goto, Y., Nonaka, I., and Hayashi, J.I. (2000). Generation of mice with mitochondrial dysfunction by introducing mouse mtDNA carrying a deletion into zygotes. *Nat. Genet.* *26*, 176–181.
19. Nakada, K., Sato, A., Sone, H., Kasahara, A., Ikeda, K., Kagawa, Y., Yonekawa, H., and Hayashi, J. (2004). Accumulation of pathogenic DeltamtDNA induced deafness but not diabetic phenotypes in mito-mice. *Biochem. Biophys. Res. Commun.* *323*, 175–184.
20. Fan, W., Waymire, K.G., Narula, N., Li, P., Rocher, C., Coskun, P.E., Vannan, M.A., Narula, J., Macgregor, G.R., and Wallace, D.C. (2008). A mouse model of mitochondrial disease reveals germline selection against severe mtDNA mutations. *Science* *319*, 958–962.
21. Li, J., Zhou, K., Meng, X., Wu, Q., Li, S., Liu, Y., and Wang, J. (2008). Increased ROS generation and SOD activity in heteroplasmic tissues of transmitochondrial mice with A3243G mitochondrial DNA mutation. *Genet. Mol. Res.* *7*, 1054–1062.
22. Vempati, U.D., Torraco, A., and Moraes, C.T. (2008). Mouse models of oxidative phosphorylation dysfunction and disease. *Methods* *46*, 241–247.
23. Tyynismaa, H., and Suomalainen, A. (2009). Mouse models of mitochondrial DNA defects and their relevance for human disease. *EMBO Rep.* *10*, 137–143.
24. Bacman, S.R., Kauppila, J.H.K., Pereira, C.V., Nissanka, N., Miranda, M., Pinto, M., Williams, S.L., Larsson, N.G., Stewart, J.B., and Moraes, C.T. (2018). MitoTALEN reduces mutant mtDNA load and restores tRNA(Ala) levels in a mouse model of heteroplasmic mtDNA mutation. *Nat. Med.* *24*, 1696–1700.
25. Gammage, P.A., Viscomi, C., Simard, M.L., Costa, A.S.H., Gaude, E., Powell, C.A., Van Haute, L., McCann, B.J., Rebelo-Guiomar, P., Cerutti, R., et al. (2018). Genome editing in mitochondria corrects a pathogenic mtDNA mutation in vivo. *Nat. Med.* *24*, 1691–1695.
26. Mok, B.Y., de Moraes, M.H., Zeng, J., Bosch, D.E., Kotrys, A.V., Raguram, A., Hsu, F., Radey, M.C., Peterson, S.B., Mootha, V.K., et al. (2020). A bacterial cytidine deaminase toxin enables CRISPR-free mitochondrial base editing. *Nature* *583*, 631–637.
27. Guo, J., Zhang, X., Chen, X., Sun, H., Dai, Y., Wang, J., Qian, X., Tan, L., Lou, X., and Shen, B. (2021). Precision modeling of mitochondrial diseases in zebrafish via DdCBE-mediated mtDNA base editing. *Cell Discov.* *7*, 78.
28. St John, J.C., Facucho-Oliveira, J., Jiang, Y., Kelly, R., and Salah, R. (2010). Mitochondrial DNA transmission, replication and inheritance: a journey from the gamete through the embryo and into offspring and embryonic stem cells. *Hum. Reprod. Update* *16*, 488–509.
29. Shoubridge, E.A., and Wai, T. (2007). Mitochondrial DNA and the mammalian oocyte. *Curr. Top. Dev. Biol.* *77*, 87–111.
30. Thundathil, J., Filion, F., and Smith, L.C. (2005). Molecular control of mitochondrial function in preimplantation mouse embryos. *Mol. Reprod. Dev.* *71*, 405–413.
31. Lee, H., Lee, S., Baek, G., Kim, A., Kang, B.C., Seo, H., and Kim, J.S. (2021). Mitochondrial DNA editing in mice with DddA-TALE fusion deaminases. *Nat. Commun.* *12*, 1190.
32. Zhang, H., Burr, S.P., and Chinnery, P.F. (2018). The mitochondrial DNA genetic bottleneck: inheritance and beyond. *Essays Biochem.* *62*, 225–234.
33. Taylor, R.W., Giordano, C., Davidson, M.M., d'Amati, G., Bain, H., Hayes, C.M., Leonard, H., Barron, M.J., Casali, C., Santorelli, F.M., et al. (2003). A homoplasmic mitochondrial transfer ribonucleic acid mutation as a cause of maternally inherited hypertrophic cardiomyopathy. *J. Am. Coll. Cardiol.* *41*, 1786–1796.
34. Liu, Q., Wang, C., Jiao, X., Zhang, H., Song, L., Li, Y., Gao, C., and Wang, K. (2019). Hi-TOM: a platform for high-throughput tracking of mutations induced by CRISPR/Cas systems. *Sci. China Life Sci.* *62*, 1–7.